Eur Biophys J (1996) 25: 67–73

BIOPHYSICS LETTER

T. Schröder · Th. Schürholz

Bimodal solubilization of phospholipid-cholesterol vesicles in 3-[(3-cholamidopropyl)dimethylammonio]-1-propanesulfonate (CHAPS) solutions. Formation of filamentous and helical microstructures depends on negatively charged lipids

Received: 28 May 1996 / Accepted: 26 July 1996

Abstract Phospholipid/cholesterol vesicles were solubilized by 3-[(3-cholamidopropyl)dimethylammonio]-1-propanesulfonate (CHAPS). Above 30 mol% cholesterol (Ch) in the lipid vesicles several remarkable changes of the solubilization process were observed. (i) Two modes of solubilization: The effective detergent to lipid ratio $R^c(M)$ for the formation of mixed micelles decreased from $R^c(M) = 43 \pm 3$ at low lipid concentrations, $[L] \leq 0.15$ mM, to $R^c(M) = 2.4 \pm 0.3$ above $[L] = 0.5$ mM (40 mol% Ch, $T = 20$ °C). (ii) At subsolubilizing CHAPS concentrations, filamentous and helical microstructures were formed, similar to those which were observed in native and model bile. (iii) The number of observed fibers was about two orders of magnitude higher in the presence of the negatively charged lipids phosphatidylglycerol (PG) and phosphatidic acid (PA) compared to the zwitterionic phosphatidylcholine (PC). Fiber formation began after 16–18 h using PG and PA compared to 3–4 days in the presence of PC. Screening of the charged lipids by NaCl effectively reduced the formation of fibers. Assuming binding of Na^+ to the charged lipid aggregates, an intrinsic binding constant $K_{int} = 0.6\ M^{-1}$ was determined by applying the Gouy-Chapman theory. After the addition of CHAPS to PG/Ch vesicles, a fast initial solubilization of the vesicles (<1 min) to mixed micelles ($r_h = 2.3 \pm 0.2$ nm) and small vesicles ($r_h = 23 \pm 1$ nm) was observed, followed by an intermediate period of 2 h, after which the formation of fibers occurred (>15 h). The microstructures are visualized by darkfield and electron microscopy. The method of vesicle solubilization is compared to the dilution of concentrated micellar solutions, which is usually applied to model bile systems.

Key words Gallstone · Cholesterol monohydrate crystals · Phase separation · Light scattering · Electron microscopy

T. Schröder · Th. Schürholz (✉)
Department of Biophysical Chemistry, University of Bielefeld, D-33615 Bielefeld, Germany (Fax: +49-521 106 6146)

Abbreviations CHAPS 3-[(3-cholamidopropyl)dimethylammonio]-1-propanesulfonate · Ch cholesterol · $[D_T]^c$ critical concentration of (total) detergent · $[D_w]^c$ critical concentration of detergent in water · PA phosphatidic acid · PC phosphatidylcholine · PG phosphatidylglycerol · $R^c(M)$ critical detergent to lipid ratio in the micelles · TC taurocholate

Introduction

The formation of cholesterol monohydrate crystals in the bile is known to be the main cause of gallstone disease (Salen and Tint 1989; Donovan and Carey 1991). The low solubility of cholesterol in bile acid solutions is considerably improved by addition of phospholipid (PL) and has been shown to depend critically on the nature of the bile acids and the PL species in model bile systems (Bourgès et al. 1967; van de Heijning et al. 1994; Mazer et al. 1980; Liu et al. 1994). In native and in model bile systems micellar as well as vesicular aggregates were found (Mazer et al. 1980). In bile supersaturated with cholesterol the formation of cholesterol monohydrate crystals was observed. Recently it has been shown that several metastable intermediate structures are involved in cholesterol crystallization, including filamentous, helical and tubular structures (Konikoff et al. 1992; Chung et al. 1993; Konikoff et al. 1994). Cholesterol, as well as the bile acid derivative CHAPS, are frequently used for membrane protein solubilization and reconstitution. Addition of cholesterol to PL-vesicles increases the minimal concentration of CHAPS, which is necessary for vesicle solubilization (Schürholz 1996). Here we show the formation of fibers and helical superstructures in the presence of CHAPS, phospholipid and cholesterol and its dependence on the lipid and salt composition.

Material and methods

Soybean phosphatidylglycerol 99% (PG), soybean phosphatidic acid 99% (PA), and soybean phosphatidylcholine 99% (PC) were purchased from Lipoid KG. 3-[(3-cholamidopropyl)-dimethylammonio]-1-propanesulfonate (CHAPS), cholesterol (Ch), and bile salts were purchased from SIGMA. All chemicals were used without further purification.

Preparations

Vesicles were prepared with the aid of an extruder as described earlier (Schürholz 1996). Polycarbonate filter with pore sizes of 100 nm were used for dynamic light scattering measurements and 400 nm for all other measurements. To analyze vesicle solubilization, CHAPS was added at different concentrations and the samples were incubated as indicated in the text. Solubilization of liposomes was monitored by light scattering (at an angle of 90°, and at wavelength, $\lambda = 500$ nm) in a Hitachi F4010 spectrofluorimeter. To determine the bound detergent (D_b) to lipid (L) ratio $R^c(M) = [D_b]/[L]$ in the micelles, different lipid concentrations were used (0.04–16 g/L total lipid). The standard incubation time was 1 day, which is generally sufficient for PL-vesicle solubilization.

Alternatively, cholesterol crystal formation was studied using the dilution method as described by Konikoff et al. (1992). In brief, detergents, PLs and Ch were co-precipitated from $CHCl_3$:MeOH (2:1) at a molar ratio of 97.5 : 0.8 : 1.7 for taurocholate, 97.6 : 0.8 : 1.6 for cholate and 94.3 : 1.8 : 3.9 for CHAPS. The precipitate was redissolved in aqueous buffer, 10 mM HEPES, pH 7.4, 150 mM NaCl, 3 mM NaN_3 at 70 g/L and diluted 6 fold. All ratios and %-values here and in the other sections are molar quantities.

Dynamic light scattering

Dynamic light scattering measurements were performed in the VV geometry; vertical polarization of the incident beam and detection of the vertically polarized scattered light. The light source was an argon iron laser (Coherent; Model Innova 90-5) in single mode, operating at $\lambda = 488$ nm. The laser power was optically stabilized at 300 mW. Intensity autocorrelation functions were measured at a temperature of 20 °C at scattering angles from 30° up to 140°. The scattered light was processed through an ALV 5000 multiple tau correlator. Inverse Laplace transformation of the normalized electric field autocorrelation function, as provided by CONTIN, was used to calculate the relaxation rates (Droegemeier et al. 1996).

Darkfield microscopy

Darkfield microscopy was carried out with a Olympus BH2 microscope equipped with an oil immersion darkfield condenser (n.a. 1.3) using either a 10× or a 40× objective. The micrographs were taken with an OM-2 camera using a 2.5× projection lens and flash light illumination.

Electron microscopy

The samples were diluted to about 0.5 mg/mL of lipid and negatively stained as described earlier (Schürholz et al. 1992). The samples were viewed at 50 kV in a Zeiss TEM-109 electron microscope.

Results

The changes in the light scattering intensity (I_{LS}) as a function of the CHAPS concentration in Fig. 1 indicate size changes and particle conversions. The particle conversions may be analyzed in terms of lyotropic phase transitions (Schürholz et al. 1989; Schürholz 1996). At a critical CHAPS concentration $[D_T]^c$, I_{LS} reached a low and constant value indicating complete solubilization of vesicles (breakpoint C). At this stage the lipids were solubilized in small mixed micelles of average hydrodynamic radius $r_h = 2.3 \pm 0.2$ nm, as determined by dynamic light scattering. If the law of mass conservation is applied to this critical point, we obtain (Schürholz et al. 1989):

$$[D_T]^c = [D]^c + R^c \times [L] \quad (1)$$

where $[D]^c$ is a transition constant, which can be the critical concentration of free detergent $[D_w]^c$. $R^c = [D_b]/[L]$ is the critical ratio of bound detergent in the particles, here the mixed micelles (M). It should be noted that R^c is an average quantity and that micelles with different lipid composition and R^c value may coexist (see results below). Since the concentration of free lipid is very low, the concentration of lipid in the micelles and vesicles [L] was approximated by the total lipid concentration. For pure PG-vesicles breakpoint C corresponded to $R^c(M) = 0.44$ and a concentration of free detergent $[D_w]^c = 0.45$ mM (CMC = 4 mM for pure CHAPS). When Ch was added to the lipid, $R^c(M)$ increased with increasing Ch content up to $R^c(M) = 0.7$ at 30% Ch.

Above 30% Ch the solubilization curves show first a marked minimum at breakpoint A followed by a maximum, breakpoint B. The peak was highest at 60% Ch. At even higher Ch contents, Ch precipitated during vesicle formation. In addition, $R^c(M)$ increased markedly above 30% Ch. Data representation with Eq. (1) indicates a transition from one mode of CHAPS binding (or micelle formation) to another one at $[L] \approx 0.2$ mM (Fig. 2). For a 6 : 4 mixture of PG and Ch, and for $[L] \leq 0.15$ mM, a value of $R^c(M) = 43 \pm 2$ was determined. The intercept yields $[D]^c = 4.5 \pm 0.2$ mM (data group labeled C in Fig. 2), which is a little higher than the CMC = 4 mM of the pure detergent CHAPS. At higher lipid concentrations, $R^c(M)$ decreased to the (final) value of $R^c(M) = 2.4$ (0.5 mM $\leq [L] \leq$ 16 mM). Similar transitions of R^c are seen for breakpoints

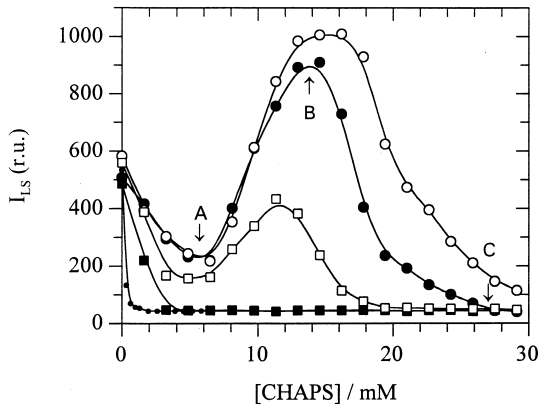

Fig. 1 Solubilization curves of phosphatidylglycerol/cholesterol vesicles (0.5 g/L, 1 d). Light scattering intensity I_{LS} (90°, λ=500 nm) as a function of the CHAPS concentration in 10 mM HEPES, pH 7.4, T=293 K, 150 mM NaCl. The cholesterol (Ch) content is given in mol% of total lipid: · 0%, ■ 10%, □ 40%, ● 50%, ○ 60%. The breakpoints *A*, *B* and *C* denote the minimum, maximum and complete solubilization of the vesicles (50% Ch). Between breakpoint A and C 2 macroscopic phases exist at equilibrium (Ch monohydrate crystals and a micellar-vesicular phase)

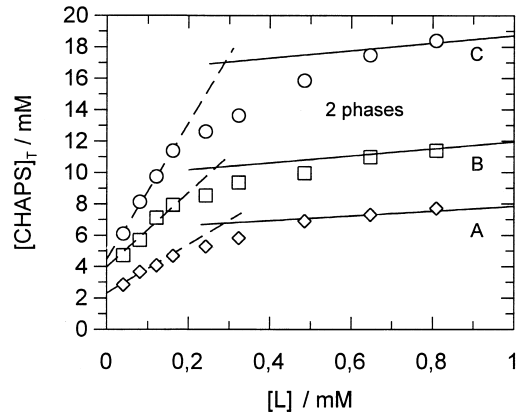

Fig. 2 Detergent-lipid phase diagram. The critical total CHAPS concentration $[CHAPS_T]^c$ at breakpoints *A* (◇), *B* (□) and *C* (○) as a function of the total lipid concentration [L]. The strong decrease in the slope ($R^c=[D_b]/[L]$) at [L]≈0.2 mM indicates a lyotropic phase transformation. The solid lines are based on data, which extend up to [L]=16 mM; these data are not shown for a higher resolution of the transition region. At [L]>1 mM $[CHAPS]_T$ is a linear function of [L]

A and B at [L]≈0.2 mM in Fig. 2. Here mixed micelles coexist with vesicles or crystalline structures (see below) and the slopes reflect the average composition of all particles. At breakpoint A (minimum) the partially solubilized vesicles had a hydrodynamic radius of $r_h=23\pm1$ nm compared with $r_h=54\pm1$ nm before addition of detergent. At 37 °C higher CHAPS concentrations were needed for complete solubilization (breakpoint C) and R^c was determined as $R^c(M)=3.6$ (0.5 mM≤[L]≤16 mM).

Since the maximum in the solubilization curve was indicative of the formation of larger particles, the samples were further analyzed by microscopy. In the darkfield microscope long fibers and helical ribbons were observed (Fig. 3). In samples which corresponded to the right hand side of the light scattering maximum in Fig. 1 (towards higher CHAPS concentrations), small crystalline platelets were more frequently seen. The aggregate structure depended on the temperature and the time of incubation. At 20 °C, fibers were the dominating structure. At higher temperatures more and more helices developed, which eventually transformed into tubes and platelike crystals (Fig. 3d–g). The helices had different diameters and pitches without obvious preferences. The average diameter of the helices increased with time up to 10 μm. At 5 °C the microstructures, thin filaments and rods were aggregated in clusters, also after transformation into transparent crystals (Fig. 3a, b). The rods could be spotted by plaques of milky-white appearance. After 1–2 weeks only Ch crystals, vesicles, and micelles were left, independent of the incubation temperature.

To obtain more structural information on the fibers, negative stained samples were viewed in the electron microscope. The electron micrograph (Fig. 4) shows fibers of 90 nm diameter. In addition, a ribbon of 500 nm width can be observed. At one site the ribbon is folded and shows its narrow side. It is seen that the thickness of the ribbon compares well with the diameter of the fibers. The material, which is adsorbed to the fibers probably stems from vesicles or mixed micelles. It is possible that the adsorption is at least in part an artifact induced by the staining process.

To analyze the initial events of filament formation the optical density (OD) of the solution at breakpoint B was measured as a function of time after the addition of CHAPS (for details see legend to Fig. 5). Three kinetic phases could be distinguished: (i) A fast solubilization of the vesicles with a half-life of 0.5 min. (ii) an intermediate period of about 2 hours of apparently no change in the particle size and (iii) a strong increase in OD indicating the beginning of filament formation. In contrast to Ch monohydrate crystal formation (broken line), the formation of filaments with time appears to be non-monotonous; the point of inflection is at t≈3 h. In the darkfield microscope the first filaments were seen after 16 h.

It was expected that the formation of the filamentous microstructures depended on either the negative charge of PG or on its bulky head-group. PG was exchanged by phosphatidic acid (PA), which is a charged but less hydrophilic lipid with a small head-group. Surprisingly, with PA the same structures and the same temperature dependence were found. When PG was increasingly replaced by PC, the formation of fibers at 20 °C was drastically reduced above 30% PC in the PL moiety. The importance of charge was further analyzed by the addition of salt to the vesicle suspension. In Fig. 6 it is seen that the maximum (breakpoint B) is already considerably reduced at 150 mM NaCl. The half maximal value of I_{LS} can be evaluated as $[NaCl]_{0.5}\approx80$ mM (see also Discussion).

Since filamentous microstructures had been observed first in model bile systems containing the uncharged lipid PC, PC and the bile acids cholate and taurocholate were

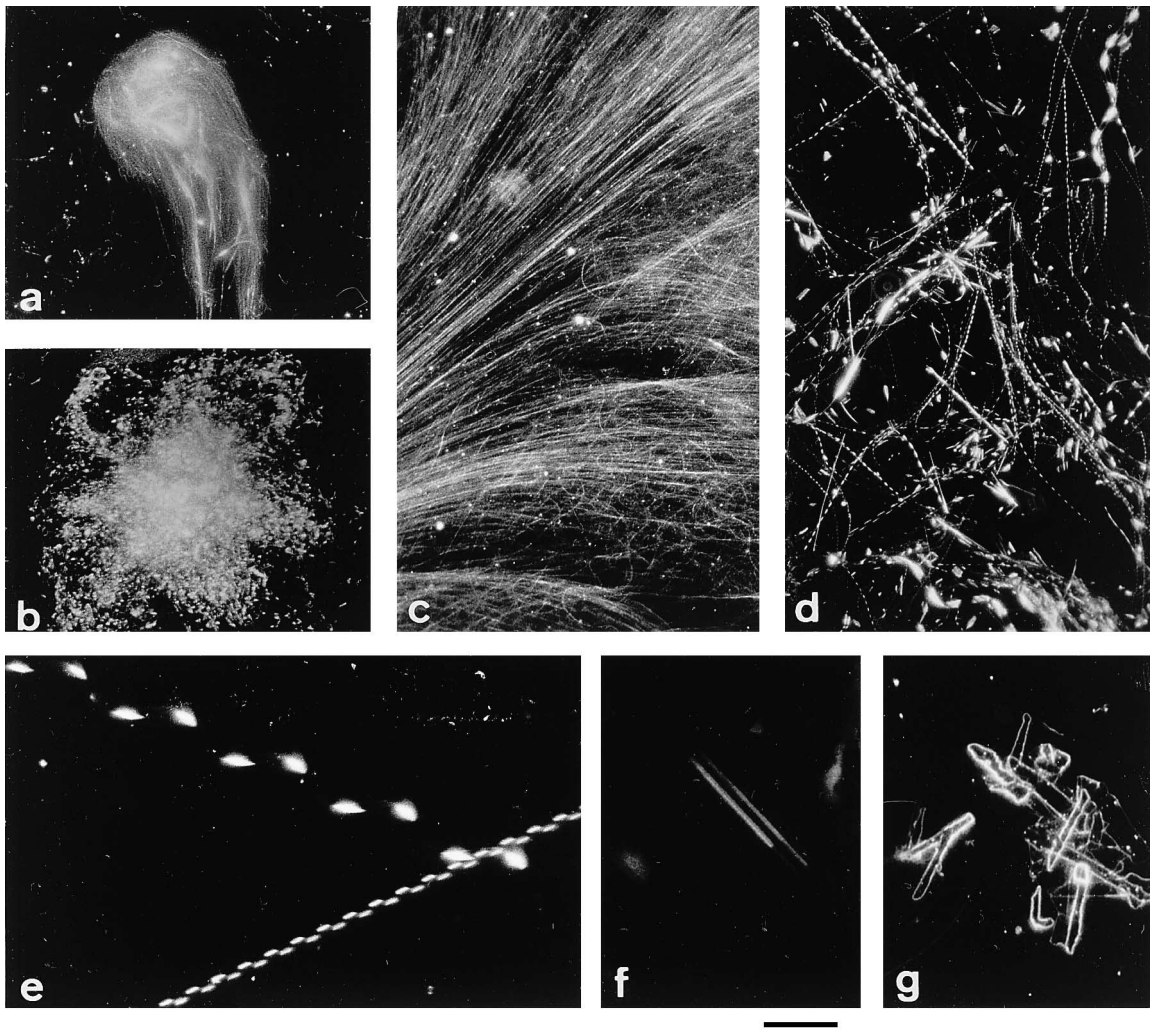

Fig. 3a–g Darkfield micrographs of various intermediate structures found during cholesterol crystal formation. At 5 °C (**a**, **b**) thin filaments and short rods are seen, which are clustered in aggregates and networks; at 20 °C predominantly long fibers are formed (**c**), whereas at 37 °C helices become the dominant structure (**d**, **e**); incubation for several days finally leads to the development of crystalline tubes and plates (**f**, **g**), independent of the temperature. The bar corresponds to 100 μm (**d**) and 25 μm (all others)

included in the investigations. In addition to vesicle solubilization, we also applied the dilution method, which has been used to test model bile systems (Konikoff et al. 1992). The observation time was extended to 1 week. In the concentrated bile salt/CHAPS solution, which is used for the dilution method, Ch can be solubilized at higher Ch : PG (or PC) ratios than in vesicles. By dilution, the surfactant solution becomes supersaturated with cholesterol and consequently cholesterol is precipitated. The results are summarized in Table 1. The formation of fibers and helices after dilution of a micellar solution did not markedly differ from the vesicle solubilization method. Fibers and helices were obtained at similar final surfactant compositions.

The concentration of CHAPS, at which fiber formation was observed, was [CHAPS]=9 mM compared to 21 mM

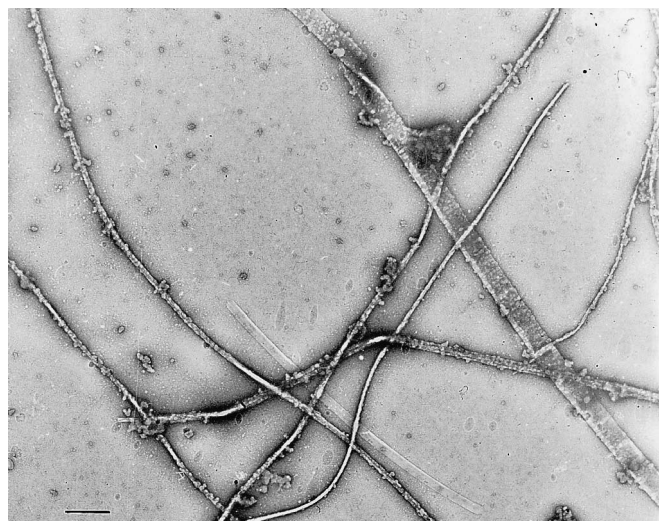

Fig. 4 Negative stain electron micrograph of the filaments. The lipid concentration was [L]=0.5 g/L in 10 mM HEPES (pH 7.4) and 150 mM NaCl. The bar indicates 1 μm

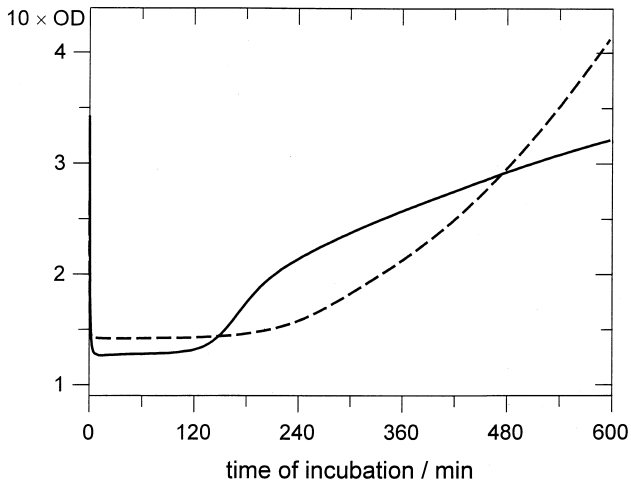

Fig. 5 Kinetics of vesicle solubilization and filament formation. The optical density (OD) at $\lambda = 500$ nm of the vesicle suspension ([L] = 2 g/L) after addition of CHAPS as a function of time. The decay in OD reflecting fast vesicle solubilization (half-life ≈ 30 s) is followed by an intermediate period of only small OD change. The OD increases again after 2 h indicating the first stages in the formation of larger structures. The full line corresponds to breakpoint B in Fig. 1 (filaments), the broken line corresponds to a composition intermediate between breakpoint B and C (mainly Ch monohydrate platelet formation)

Table 1 Microstructure formation as a function of lipid, detergent composition and temperature T. Only the predominant structures are given. The upper case number by the name of the structure indicates the relative number of the microstructures on a logarithmic scale (10^x) as evaluated from microscope observations. τ denotes the time for the beginning of microstructure formation. The standard concentration of total lipid was 0.5 g/L, but higher concentrations were also used. The cholesterol content of the lipid was 40% and 50% in the solubilization experiments, and 70% in the dilution method

Lipid	Detergent	T/°C	τ	Structure
A. Vesicle solubilization				
PG	CHAPS	5	1 d	Cluster^2
PG	CHAPS	20	18 h	Fibers^2
PG	CHAPS	37	16 h	Helices^2
PC	CHAPS	5	5–6 d	Crystals^0
PC	CHAPS	20	3–4 d	Fibers^0
PC	CHAPS	37	1 d	Tubes, helices^0
PG	TC	20	4–5 d	Fibers, helices^0
PG	Cholate	20	6–7 d	Fibers, helices^0
PC	TC	20	2–3 d	Helices$^{0.5}$
B. Dilution method				
PG	CHAPS	37	≤1 d	Helices, fibers^2
PC	CHAPS	37	1–2 d	Helices, fibers^0
PC	TC	37	2 d	Helices, fibers^0

for the bile salts (0.17 mM PL, 0.37 mM Ch). The development of the filamentous and helical structures was much slower in the presence of PC compared to PG and PA (see Table 1). However, the different velocities of fiber formation after sample dilution were not so pronounced as seen with the vesicle solubilization method. In addition, the number of the microstructures evaluated from darkfield microscopy was about 2 orders of magnitude lower when PC was used. Correspondingly, no light scattering maximum was seen in the solubilization curve (not shown). The highest yield of fibers with PC as phospholipid component was obtained in the presence of taurocholate.

Discussion

The formation of filamentous structures in the quaternary system "water, cholesterol, phospholipid and CHAPS" compares well with the development of cholesterol crystals in model bile systems (Konikoff et al. 1992): Addition of bile salt to PL/Ch vesicles results in the gradual formation of mixed micelles (Stolk et al. 1994). The partial solubilization of vesicles is indicated here by the initial decrease of the light scattering intensity (minimum of the solubilization curve, Fig. 1). In this process more PL than Ch is extracted from the vesicles into the mixed micelles causing an increase of the Ch/PL ratio in the vesicles (Strasberg and Harvey 1990; Cohen et al. 1990). Finally, supersaturation of Ch in the vesicles should lead to Ch crystallization and finally precipitation (Collins and Phillips 1982; Halpern et al. 1986; Lamont and Carey 1992). The minimal detergent concentration at breakpoint A, $[D]_w(A) = 2.3$ mM, is in line with a reduced Ch/PL ratio in the mixed micelles and thus an accumulation of Ch in the vesicles ($[D]_w(C) = 4.5$ mM is necessary for complete solubilization). In addition, the extraction of lipid from the vesicles into mixed micelles is reflected in the reduction of the vesicle radius from $r_h = 54$ nm to $r_h(A) = 23$ nm at breakpoint A. Calorimetric and X-ray measurements showed a lower miscibility of Ch with PG compared to Ch with PC (Borochov et al. 1995). Thus phase separation may be induced in PG-Ch vesicles at a lower Ch content. In general, the detergent concentration, which is needed for the solubilization of natural phospholipids is a linear function of the lipid concentration (Eq. (1)) (Ollivon et al. 1988; Paternostre et al. 1988; Schürholz 1996). Here, above 30% Ch in the lipid (at least) two domains can be distinguished in the phase diagram (Fig. 2) with respect to R^c. The high value of $R^c = 43$ at low lipid concentrations reflects the poor miscibility of Ch with bile acids and its derivatives. The about 20 fold decrease of R^c at $[L] > 0.2$ mM is expected to correlate with a reorganization of the colloidal structure. However, below 0.2 mM lipid the light scattering intensity was to low to analyze the particle size by correlation spectroscopy. Yet, the hydrodynamic radius $r_h = 2.3$ nm of the mixed micelles at $[L] = 0.8$ mM is close to the value of pure CHAPS micelles ($r_h = 1.8$–2.1 nm). Assuming that the mixed micelles at $[L] < 0.2$ mM are not smaller than the

pure CHAPS micelles, a possible aggregation at higher lipid concentrations therefore would not exceed double the initial molecular mass of the mixed micelle.

A sequence of intermediate structures was observed in model bile systems supersaturated with cholesterol, instead of direct cholesterol monohydrate crystal formation as was initially proposed (Konikoff et al. 1992; Chung et al. 1993). The sequence fibers, helices, tubules and crystal plates matches perfectly the structures, which were found here upon solubilizing PG/Ch vesicles with the zwitterionic detergent CHAPS. However, the high yield of fibers and the requirement of negatively charged lipids is obviously a peculiarity of CHAPS. Since the bile acids are negatively charged themselves, charge is supplied by the detergent. According to our experiments, CHAPS is more effective in Ch solubilization (>2×) than TC and cholate. A dependence of Ch solubilization on the type of steroid backbone of the bile salt (number and sites of hydroxylgroups) has also been reported (van de Heijning et al. 1994).

The dependence of fiber formation on salt concentration can be described by the dissociation of Na^+ from mixed lipid aggregates (vesicles, micelles), which serve as nuclei for fiber (F) formation:

$$A \cdot Na \rightleftharpoons A + Na^+ \xrightarrow{\text{slow}} F + Na^+ \qquad (2)$$

It is assumed that the dissociation of Na^+ from the binding site A on the lipid aggregates is an equilibrium reaction with the apparent equilibrium constant K_D. Applying mass conservation, $[A]=[A_0]-[A \cdot Na]$, the degree of salt binding Θ can be defined as

$$\Theta = \frac{[A \cdot Na]}{[A_0]} = \frac{[NaCl]}{K_D + [NaCl]} \qquad (3)$$

Assuming proportionality, $[F] \propto [A] = [A_0](1-\Theta)$ and $I_{LS} \propto [F]$ we obtain[1]

$$I_{LS} = (I_{LS}^0 - I_{LS}^\infty) \cdot \left(\frac{[NaCl]}{K_D + [NaCl]} \right) + I_{LS}^\infty \qquad (4)$$

where I_{LS}^0 and I_{LS}^∞ are the light scattering intensity at zero and high NaCl concentration, respectively. I_{LS}^∞ accounts for the basic light scattering, which is not caused by the fibers. The curve in Fig. 6b was obtained with $K_D = 76$ mM. The Gouy-Chapman approach may be applied to calculate the surface potential ψ_0 at a given salt concentration. At high electrostatic potentials ($\psi_0 \cdot e_0 > kT$) ψ_0 is given by (Cevc and Marsh 1987):

$$\psi_0 = (2\,kT/ze)\,\ln[(ze/kT)\,(\sigma_{el}\lambda/\varepsilon\varepsilon_0)]$$
$$= (-51\text{ mV})\,z^{-1}\ln(0.36\,A_c\,c^{0.5}) \qquad (5)$$

Here ze is the charge of the symmetrical electrolyte, σ_{el} the surface charge density of the lipid particle, A_c the surface area per charge in nm^2, c the electrolyte concentration

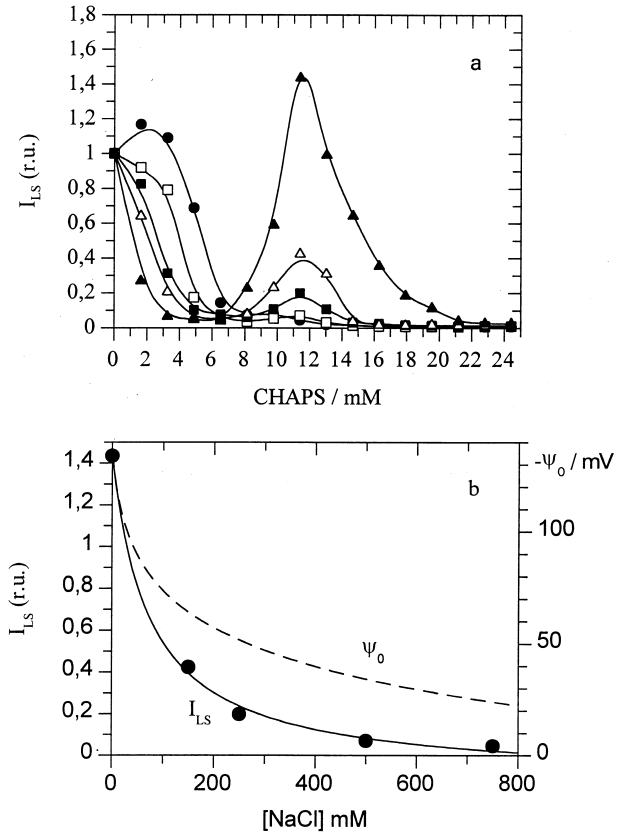

Fig. 6a, b Filament formation as a function of [NaCl]. **a** Solubilization curves of lipid vesicles (0.8 mM, PG:Ch=6:4); static light scattering intensity I_{LS} (90°, λ=500 nm, 293 K) as a function of [CHAPS] in 10 mM HEPES-Na (pH 7.4). [NaCl]: ▼ 0 mM, ▽ 150 mM, ■ 250 mM, □ 500 mM, ● 750 mM. **b** I_{LS} at the peak in **a** ([CHAPS]=11.3 mM) as a function of [NaCl]. The curve was obtained using Eq. (2) and K^{-1}=76 mM. The surface potential ψ_0 of the vesicles was calculated using Eq. (5) and a surface area of 2 nm^2/chrge (≙50% saturation)

in mol/L, k the Boltzmann constant, T the temperature, ε the relative permittivity, and ε_0 the permittivity of the vacuum. At 50% saturation of the Na^+-binding sites A_c can be estimated as $A_c = 2$ nm^2. Then the surface potential is $\psi = -80$ mV, as calculated by Eq. (5). Considering the electrostatic contribution to the standard value of the free energy of association, the intrinsic association constant K_{int} can be determined as

$$K_{int} = K_D^{-1} \cdot e^{F\psi/RT} \cong 0.6\ M^{-1}. \qquad (6)$$

This value equals $K_{int} = 0.6\ M^{-1}$ for Na^+-association, which was calculated from measurements of the electrophoretic mobility of PG-vesicles (Eisenberg et al. 1979). At high salt concentrations the reduction of the headgroup hydration may also affect the structural changes.

For example, in Fig. 6A it is seen that the at high [NaCl] the vesicles are more resistant to CHAPS. The CHAPS concentration, which corresponds to $I_{LS} = 0.5 \cdot I_{LS,max}$ is shifted from [CHAPS]=1.2 mM at [NaCl]=0 mM to [CHAPS]=5.5 mM at [NaCl]=750 mM. This increased stability of the bilayer state is in line with the expected re-

[1] Under the microscope it is seen that the *number* of fibers is reduced with increasing salt concentration, the structure of the fibers is not affected. Therefore the approximation $I_{LS} \propto [F]$ is justified

duction of the effective head-group area (Seddon and Cevc 1993). Although PA has a smaller head-group than PG, the same yield of filament formation was measured. Thus, the size of the head-group seems to be of minor importance with regard to filament formation.

It has been proposed that aggregation or fusion of Ch saturated vesicles is the initial step of filament formation (Halpern et al. 1986). High surface charge and low salt concentration ar known to impede vesicle fusion. As we have shown, both conditions favor the formation of filaments. Therefore, fusion of vesicles probably is not involved in the process of filament formation. Nevertheless phase separation of Ch in Ch oversaturated vesicles may serve as nuclei for Ch crystallization.

Our results have shown that the charge of the detergent and of the lipid head group critically change the solubilization and precipitation of Ch from lipid vesicles, which is an important step in gallstone formation. In addition, the results may be used for the optimization of protein reconstitution into cholesterol containing vesicles or supported bilayers.

Acknowledgement We thank I. Goldbeck, P. Hübner and M. Barella for excellent technical assistance, Dr. W. Eimer for his support in the dynamic light scattering measurements, and Prof. E. Neumann (Bielefeld) and Dr. R. M. Warn (UEA, Norwich, England) for critically reading the manuscript. This work was supported by the Deutsche Forschungsgemeinschaft (SFB 223) and the Fonds der Chemischen Industrie.

References

Borochov N, Wachtel EJ, Bach D (1995) Phase behaviour of mixtures of cholesterol and saturated phosphatidylglycerols. Chem Phys Lipids 76:85–92

Bourgès MC, Small DM, Dervichian DG (1967) Biophysics of lipid association III. The quarternary systems lecithin-bile salt-cholesterol-water. Biochim Biophys Acta 144:189–201

Cevc G, Marsh D (1987) Phospholipid bilayers. Wiley-Interscience, New York

Chung DS, Benedek GB, Konikoff FM, Donovan JM (1993) Elastic free energy of anisotropic helical ribbons as metastable intermediates in the crystallization of cholesterol. Proc Natl Acad Sci USA 90:11341–11345

Cohen DE, Angelico M, Carey MC (1990) Structural alterations in lecithin-cholesterol vesicles following interactions with monomeric and micellar bile salts: physical-chemical basis for subselection of biliary lecithin species and aggregative states of biliary lipids during bile formation. J Lipid Res 31:55–70

Collins JJ, Phillips MC (1982) The stability and structure of cholesterol-rich codispersions of cholesterol and phosphatidylcholine. J Lipid Res 23:291–298

Donovan JM, Carey MC (1991) Physical-chemical basis of gallstone formation. Gastroenterol Clin North Am 20:47–66

Droegemeier J, Hinssen H, Eimer W (1996) Flexibility of F-Actin in aqueous solution: A study of filaments of different average length. Macromolecules 27:87–95

Eisenberg M, Gresalfi T, Riccio T, McLaughlin S (1979) Adsorption of monovalent cations to bilayer membranes containing negative phospholipids. Biochemistry 18:5213–5223

Halpern Z, Dudley MA, Kibe A, Lynn MP, Breuer AC, Holzbach RT (1986) Rapid vesicle formation and aggregation in abnormal human biles. A time-lapse video-enhanced contrast microscopy study. Gastroenterology 90:875–885

Konikoff FM, Chung DS, Donovan JM, Small DM, Carey MC (1992) Filamentous, helical and tubular microstructures during cholesterol crystallization from bile. Evidence that cholesterol does not nucleate classic monohydrate plates. J Clin Invest 90:1155–1160

Konikoff FM, Cohen DE, Carey MC (1994) Phospholipid molecular species influence crystal habits and transition sequences of metastable intermediates during cholesterol crystallization from bile salt-rich model bile. J Lipid Res 35:60–70

Lamont JT, Carey MC (1992) Cholesterol gallstone formation. 2. Pathobiology and pathomechanics. Prog Liver Dis 10:165–191

Liu CL, Jain UKJ, Lee PH, Mazer NA, Higuchi WI (1994) Cholesterol thermodynamic activity, quasielastic light scattering, and polarizing microscopy studies in aqueous taurocholate-lecithin solutions supersaturated with cholesterol. Journal of Colloid and Interface Science 165:411–424

Mazer NA, Benedek GB, Carey MC (1980) Quasielastic light scattering studies of aqueous biliary lipid systems, mixed micelle formation in bile salt-lecithin solutions. Biochemistry 19:601–615

Ollivon M, Eidelman O, Blumenthal R, Walter A (1988) Micelle-vesicle transition of egg phosphatidylcholine and octyl glucoside. Biochemistry 27:1695–1703

Paternostre M-T, Roux M, Rigaud J-L (1988) Mechanisms of membrane protein insertion into liposomes during reconstitution procedures involving the use of detergents. 1. Solubilization of large unilamellar liposomes (prepared by reverse-phase evaporation) by Triton X-100, octyl glucoside, and sodium cholate. Biochemistry 27:2668–2677

Salen G, Tint GS (1989) Nonsurgical treatment of gallstones [editorial]. N Engl J Med 320:665–666

Schürholz T, Gieselmann A, Neumann E (1989) Miscibility gap of octyl glucoside-phosphatidylcholine micellar solutions. Partition of the nicotinic acetylcholine receptor into the surfactant-rich phase. Biochim Biophys Acta 986:225–233

Schürholz T, Kehne J, Gieselmann A, Neumann E (1992) Functional reconstitution of the nicotinic acetylcholine receptor by CHAPS dialysis depends on the concentrations of salt, lipid, and protein. Biochemistry 31:5067–5077

Schürholz T (1996) The solubilization of lipid vesicles by the detergent CHAPS depends critically on the lipid composition. Functional reconstitution of the nicotinic acetylcholine receptor into preformed vesicles above the critical micellization concentrations. Biophys Chem 58:87–96

Seddon JM, Cevc G (1993) Lipid Polymorphism: Structure and stability of lyotropic mesophages of phospholipids. In: Cevc G (ed) Phospholipids Handbook. Marcel Dekker, Inc, New York, pp 403–454

Stolk MF, van de Heijning BJ, van Erpecum KJ, van den Broek AM, Renooij W, van Berge Henegouwen GP (1994) The effect of bile acid hydrophobicity on nucleation of several types of cholesterol crystals from model bile vesicles. J Hepatol 20:802–810

Strasberg SM, Harvey PR (1990) Biliary cholesterol transport and precipitation: introduction and overview of conference. Hepatology 12:1S–5S

van de Heijning BJM, Stolk MFJ, van Erpecum KJ, Renooij W, van Berge Henegouwen GP (1994) The effects of bile salt hydrophobicity on model bile vesicle morphology. Biochim Biophys Acta 203–210